



Parallel fault diagnosis using hierarchical fuzzy Petri net by reversible and dynamic decomposition mechanism

Yinhong XIANG¹, Kaiqing ZHOU^{†1}, Arezoo SARKHEYLI-HÄGELE², Yusliza YUSOFF³,
 Diwen KANG¹, Azlan Mohd ZAIN³

¹School of Communication and Electronics Engineering, Jishou University, Jishou 416000, China

²Internet of Things and People Research Center, Department of Computer Science and Media Technology, Malmö University, 20506, Malmö, Sweden

³Faculty of Computing, Universiti Teknologi Malaysia, 81310, Skudai, Malaysia

E-mail: yhxiang@stu.jjsu.edu.cn; kqzhou@jsu.edu.cn; arezoo.sarkheyli-haegel@mau.se; yusliza@utm.my; kangdiwen@jsu.edu.cn; alzanmz@utm.my

Received Mar. 12, 2024; Revision accepted Apr. 1, 2024; Crosschecked

Abstract: The state space explosion, a challenge analogous to that encountered in a Petri net, has constrained the extensive study of fuzzy Petri nets (FPNs). Current reasoning algorithms employing FPNs, which operate through forward, backward, and bidirectional mechanisms, are examined. These algorithms streamline the inference process by eliminating irrelevant components of the FPN. However, as the scale of the FPN grows, the complexity of these algorithms escalates sharply, posing a significant challenge for practical applications. To address the state explosion issue, this work introduces a parallel bidirectional reasoning algorithm for an FPN that utilizes reverse and decomposition strategies to optimize the implementation process. The algorithm involves hierarchically dividing a large-scale FPN into two sub-FPNs, followed by a converse operation to generate the reversal sub-FPN for the right sub-FPN. The detailed mapping between the original and reversed FPNs is thoroughly discussed. Parallel reasoning operations are then conducted on the left-sub-FPN and the resulting reversal right-sub-FPN, with the final result derived by computing the Euclidean distance between the outcomes from the output places of the two sub-FPNs. A case study is presented to illustrate the implementation process, demonstrating the algorithm's significant enhancement of inference efficiency and substantial reduction in execution time.

Key words: Fuzzy Petri net; State explosion; Decomposition; Parallel; Bidirectional reasoning
<https://doi.org/10.1631/FITEE.2400184>

CLC number:

1 Introduction

With the complexity of industrial manufacturing equipment and production processes increasing dramatically, a correspondingly extensive array of fault diagnosis methods has been proposed and discussed. These include the application of Petri nets (PNs) (Liu et al., 2017), deep learning techniques (Lei et al., 2020; Chen XH et al., 2021), and swarm intelligence algorithms (Ziani et al., 2017; Chen RH et al., 2020; Ye et

al., 2023). As a distinctive tool within the knowledge-driven approach, the FPN has been widely utilized for modeling, simulating, and executing diagnostic tasks within complex manufacturing systems, leading to fruitful results. This is primarily attributable to two key characteristics of FPNs (Zhou and Zain, 2016; Seatzu, 2019; Liu et al., 2022; Wang et al., 2022). Firstly, the FPN maintains the PN's ability to describe asynchronous concurrency and provides a graphical representation. Secondly, it offers a formal modeling approach for managing fuzzy and uncertain information within knowledge-based systems. This sets FPN apart from

[†] Corresponding author

the opacity and black-box nature of deep learning, as FPNs can explicitly describe the states, events, and transitions within the system, thereby enhancing the interpretability and explainability of the inference process (Rudin, 2019). More recently, more high-level PNs with fuzzy factors have been introduced to represent knowledge effectively and accommodate the diverse constraints inherent in real engineering issues. Notable examples include linguistic probabilistic linguistic PNs (Shi et al., 2024), Z-number Petri nets (Shi et al., 2022), spherical linguistic Petri nets (Mou et al., 2022), and linguistic Petri nets (Liu et al., 2022).

As knowledge-based systems increase in size, their corresponding FPNs also grow in scale (Zhou et al., 2019). This scaling phenomenon, known as the state explosion problem, poses a substantial challenge to the construction and application of FPNs (Valmari, 1998; Grobelna and Karatkevich, 2021). To address the state explosion problem, researchers have developed a suite of decomposition algorithms and reasoning techniques. These methods ensure that the resulting sub-PNs preserve the consistency of the original PN, thereby reducing the model's scale. Chen (2000) proposed a fuzzy AND/OR graph via FPN backward reasoning, which constructs an AND/OR graph from target places and reduces the model size. This approach also allows for the flexible evaluation of the truth degree for any user-specified proposition. Zaitsev (2004) discussed functional sub-PNs based on structural properties and presented a decomposition algorithm of polynomial complexity $O(n^3)$ that maintains the properties of the original PN. Lakos and Petrucci (2011) introduced a modular PN with dynamic priorities, considering transitions and the current marking rather than just the firing mode. Their approach modularizes the state space, thereby solving the state space explosion problem. Zeng et al. (2012) employed time-scale decomposition to reduce the state space in continuous-time Markov chains and decomposed stochastic PN into several sub-level models with consistent transition rates. Liu et al. (2013) introduced a fault diagnosis and cause analysis model that utilizes fuzzy evidence inference within a dynamic adaptive FPN. The model achieves reverse-cause analysis through a reverse operation and enhances fault diagnosis accuracy by integrating fuzzy evidence inference into the FPN framework.

Nishi and Matsumoto (2013) proposed a method for decomposing large-scale PNs into multiple sub-PNs capable of capturing the behavior of each system component. This method reduces the computational complexity of discovering near-optimal scheduling solutions, enhances solution efficiency, guarantees the prevention of deadlocks, and facilitates the achievement of acyclic scheduling. Shen et al. (2013) proposed a method for solving the state explosion problem of PN using matching theory. This method reduces the PN by fusing transitions with maximum weight values and eliminating redundant positions, resulting in a compressed and reduced PN. Salum (2015) introduced a novel PN analysis tool, the superposition chain, which employs superposition operators to define triggering semantics. This allows transitions to be fired in any order through superpositions, enabling the superposition chain to define an acyclic PN that can be checked in parallel or via superpositions, thus avoiding state explosion and enhancing the efficiency of PN analysis. Zhou et al. (2015a) discussed a bidirectional decomposition algorithm to divide a large-scale FPN into a series of sub-FPNs. However, the practical application of this approach is challenged by the difficulty of implementing inference on each sub-FPN. Subsequently, they developed a bidirectional adaptive inference algorithm based on intrinsic inference paths (Zhou et al., 2018) to overcome the state explosion problem by managing the dimensions of the operation matrix. Despite this advancement, the proposed bidirectional reasoning still predominantly operates with forward inference on the original FPN and backward reasoning on the simplified FPN, which means it does not employ an accurate parallel reasoning mechanism. Bai et al. (2023) introduce a decomposition algorithm for the q-rung orthopair fuzzy reversed PN, using place and transition vectors. This algorithm is able to avoid interference from unrelated propositions and decrease the complexity of inference. Yang (2023) addresses the state explosion issue of PN by proposing a polynomial decomposition algorithm via P-invariants. This algorithm decomposes complex workflow network models into simple subnet classes, which are effective for describing the process of business case handling.

Researchers focusing on inference in large-scale FPNs commonly employ various mechanisms to

simplify the original FPN and enhance reasoning efficiency. These mechanisms include using forward or backward search to identify the most straightforward reasoning path between input and output places (Jiang et al., 2022). The core of this approach is the individual implementation of forward and backward inference mechanisms. Although backward reasoning from output places can effectively capture inner inference paths and directly reduce the complexity of the matrices involved in the forward reasoning operation, the overall complexity remains substantial. In contrast, actual bidirectional reasoning involves executing simultaneous forward and backward reasoning—one starting from the initial state and the other from the goal state—with the expectation that they will converge in the middle (Russell and Norvig, 2009). However, at the current stage, the bidirectional reasoning approach fails to meet the demand for parallelism. Thus, it can be considered a hybrid reasoning technique that integrates forward and backward reasoning. Moreover, when evaluated from a parallel perspective in knowledge reasoning, the existing FPN inference method does not comply with the criteria for a ‘true’ bidirectional reasoning method.

Building on the above findings, this paper introduces a parallel bidirectional reasoning approach utilizing a hierarchical FPN enabled by a reversible and dynamic decomposition mechanism (PBR-HFPN-RDD). This method aims to achieve parallel fault diagnosis and mitigate the state explosion issues encountered in the following aspects:

1. By analyzing the clear mapping relationship between an FPN and its reverse (Re-FPN) elements, this paper delves into the Re-FPN generation algorithm and associated concepts in depth.

2. By exploring potential reasoning error sources, this paper develops a dynamic decomposition algorithm to partition two sub-FPNs of varying scales by leveraging the properties of the incidence matrix.

3. The PBR-HFPN-RDD is applied to conduct parallel reasoning operations on the derived left-sub-FPN and the reversed FPN, utilizing the obtained right-sub-FPN to achieve the final diagnosis result.

Furthermore, a case study is conducted to validate the correctness of the proposed PBR-HFPN-RDD. The experimental results indicate that PBR-HFPN-RDD can diminish the scale of ma-

trix operations within the FPN reasoning process, thereby mitigating the state explosion issue and enhancing the efficiency of model reasoning.

The remainder of this manuscript is structured as follows. Section 2 revisits the relevant concepts, including FPN, fuzzy production rules, formal inference mechanisms, and the properties of the incidence matrix. Section 3 investigates the mapping relationship between the original FPN and its corresponding reversed FPN, and introduces the algorithm for generating the reversed FPN. Section 4 analyzes the potential sources of reasoning error in a parallel fault diagnosis algorithm utilizing the reversed FPN and discusses a dynamic decomposition algorithm that segments the entire FPN, along with a detailed presentation of the PBR-HFPN-RDD. Section 5 demonstrates the feasibility and correctness of the proposed PBR-HFPN-RDD through a case study. Finally, Section 6 provides a summary of the entire paper.

2 Related Notions

This section reviews the fundamental definitions of an FPN, a fuzzy production rule (FPR), and their related notions based on the references (Yeung and Ysang, 1998; Chen SM, 2002; Zhou et al., 2015b; Yu et al., 2023).

2.1 Fuzzy Petri Net

Definition 1 Fuzzy Petri net (FPN)

A FPN can be defined as a 9-tuple $F_{PN}(\Sigma) = (P, T, F, M, W, Th, CF, I, O)$, where:

- (1) $P = \{p_1, p_2, \dots, p_n\}$ is a finite set of places;
- (2) $T = \{t_1, t_2, \dots, t_m\}$ is a finite set of transitions;
- (3) $F \subseteq (P \times T) \cup (T \times P)$ is a set of directed arcs representing the flow relations between P and T ;
- (4) $M = (m_1, m_2, \dots, m_n)^T$ is a vector to record the truth degree of the corresponding place p_i ($i = 1, 2, \dots, n$) and $m_i \in [0, 1]$. The initial marking is denoted by M_0 ;
- (5) $W = (w_{(i,j)})_{n \times m}$ is a matrix to record the weight from p_i to t_j , $w_{(i,j)} \in [0, 1]$;
- (6) $Th = (\mu_1, \mu_2, \dots, \mu_m)^T$ is a vector to record each transition's threshold t_j ($j = 1, 2, \dots, m$) and $\mu_j \in [0, 1]$

(7) $CF=(CF_{ij})_{n \times m}$ is a matrix to record each certainty factor from t_j to p_i , $CF_{ij} \in (0,1]$, ($i=1,2,\dots,n; j=1,2,\dots,m$);

(8) $I=(I(p_i,t_j))_{n \times m}$ is an input matrix, where $I(p_i,t_j)$ ($i=1,2,\dots,n; j=1,2,\dots,m$) represents a directed arc exists from p_i to t_j , $I(p_i,t_j)=w_{(i,j)}$. Otherwise, $I(p_i,t_j)=0$;

(9) $O=(O(p_i,t_j))_{n \times m}$ is an output matrix, where $O(p_i,t_j)$ represents a directed arc exists from t_j to p_i , $O(p_i,t_j)=CF_{ij}$ ($i=1,2,\dots,n; j=1,2,\dots,m$). Otherwise, $O(p_i,t_j)=0$.

Definition 2 Pre-set and post-set

For an FPN, $\bullet x = \{y | (y,x) \in F\}$ is the pre-set of x , and $x^\bullet = \{y | (x,y) \in F\}$ is the post-set of x ($x, y \in (P \cup T)$).

Definition 3 Input place and output place

Input place is a set of places that fulfill $\{p \in P | \bullet p = \emptyset \text{ and } p^\bullet \neq \emptyset\}$; Output place is a set of places that fulfill $\{p \in P | \bullet p \neq \emptyset \text{ and } p^\bullet = \emptyset\}$.

Definition 4 Enable and fire

For a given FPN with a marking M , the transition t enables, denoted as $M \geq t$, once the property that all input places $p \in \bullet t$ fulfills the following formula (1).

$$\sum M(p_i) \times W(i,j) \geq \mu(t_j) \quad (1)$$

Once, and only if, a transition is enabled, the transition fires and produces a new marking M' , denoted as $M \geq M'$. The new marking M' could be calculated using the formula (2) below.

$$M'(p) = \begin{cases} 0, & p \in \bullet t - t^\bullet \\ (\sum M(p_i) \times w(p_i,t)) \times CF(t,p), & p \in t^\bullet - \bullet t \\ M(p), & p \notin \bullet t \cup t^\bullet \end{cases} \quad (2)$$

Definition 5 Incidence matrix

An incidence matrix H is used to represent the entire flow relationships between P and T of the FPN by formula (3).

$$h_{ij} = \begin{cases} -1, & \text{if } p_i \in I(t_j), p_i \in P, t_j \in T \\ 1, & \text{if } p_i \in O(t_j), p_i \in P, t_j \in T (i=1,2,\dots,n; j=1,2,\dots,m) \\ 0, & \text{else} \end{cases} \quad (3)$$

Definition 6 Route of place and the longest route of FPN

For a given $n \times m$ FPN, the transition string t_1, t_2, \dots, t_j can be fired in order. For a given place p , if p can obtain the token from the input place, the transition string t_1, t_2, \dots, t_j is called a route of the place p , and the length l_j of the route l of the place p is defined as $l_j = |r_j| = h_j$, where h is the number of the transitions of this route r_j .

If p is the output place, there are k routes of p from the input place r_1, r_2, \dots, r_k , and the corresponding path length of each route is l_1, l_2, \dots, l_k , respectively. The longest route of the FPN is $l_{\max} = |\max(l_1, l_2, \dots, l_k)|$.

Definition 7 Immediate reachability set and reachability set

If $p_i \in \bullet t_i$ and $p_j \in t_i^\bullet$, then p_j is called immediate reachability from p_i . The set of places that are immediately reachable from a place p_i is called the immediate reachability set of p_i and is denoted by $IRS(p_i)$. The set of places that are reachable from a place p_i is called the reachability set of p_i and is denoted by place $RS(p_i)$.

2.2 Fuzzy Production Rule

Definition 8 Fuzzy production rule (FPR): FPR is generally defined below.

If $D(\lambda)$, then $Q(CF, \mu, w)$,

where:

(1) D is a finite set of preconditions $D = \{D_1, D_2, \dots, D_n\}$;

(2) Q is a finite set of conclusions $Q = \{Q_1, Q_2, \dots, Q_n\}$;

(3) $CF \in [0,1]$ is the belief strength of a rule to indicate the confidence of the related conclusions derived by conditions;

(4) $\mu \in [0,1]$ is the threshold value of the rule;

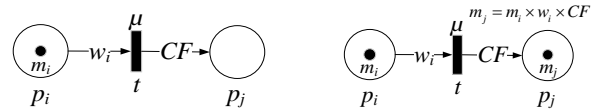
(5) $w \in [0,1]$ is the weight of each precondition.

FPR is a type of production rule that describes the interior relationship between pre-positions and conclusions with fuzzy parameters. The FPRs can be classified into three types: simple rules, "AND" rules, and "OR" rules.

(1) Simple rule

If $D(\lambda)$, then $Q(CF, \mu, w=1)$.

If $\lambda \geq \mu$ exists, then the rule can be fired. The corresponding FPN of a simple rule is generated as shown in Fig. 1(a), and the result after being fired is $m(p_j) = m(p_i) \times w_i \times CF$ (Fig. 1(b)).



(a) before transition fired (b) after transition fired

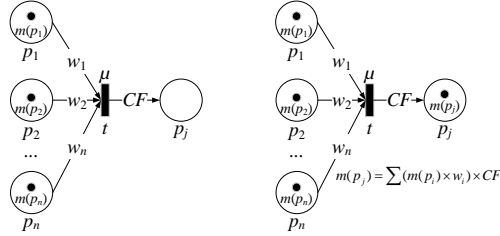
Fig. 1 FPN corresponds to the simple rule

(2) "AND" rule

If $D_1(\lambda_1)$ and $D_2(\lambda_2)$ and \dots and $D_n(\lambda_n)$, then $Q(CF, \mu, \sum w_i = 1)$.

If $\sum w_i \times \lambda_i \geq \mu$ exists, then the rule can be fired. The corresponding FPN of the "AND" rule is generated as

shown in Fig. 2(a), and the result after being fired is $m(p_j) = \sum(m(p_i) \times w_i) \times CF$ (Fig. 2(b)).



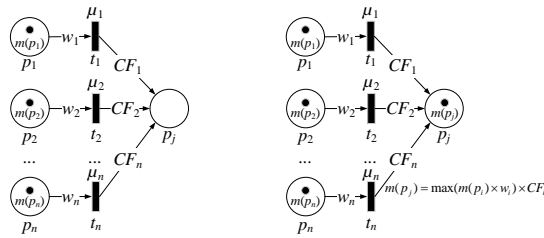
(a) before being fired (b) after being fired

Fig. 2 FPN corresponds to the "AND" rule

(3) "OR" rule

If $D_1(\lambda_1)$ or $D_2(\lambda_2)$ or \dots or $D_n(\lambda_n)$, then $Q(CF, \mu, w_i = I)$.

If $w_i \times \lambda_i \geq \mu_i$ exists, then the rule can be fired. The corresponding FPN of the "OR" rule is generated as shown in Fig. 3(a), and the result after being fired is $m(p_j) = \max(m(p_i) \times w_i) \times CF_i$ (Fig. 3(b)).



(a) before being fired (b) after being fired

Fig. 3 FPN corresponds to the "OR" rule

2.3 Incidence Matrix

An incidence matrix of a given FPN records the flow relationships between places and transitions. Specifically, the incidence matrix is used to delineate different FPRs. Consequently, the function and associated analysis of the incidence matrix are discussed below.

A specific FPN and its corresponding incidence matrix are illustrated in Fig. 4 to elucidate the concept. The incidence matrix H corresponding to Fig. 4 is obtained below.

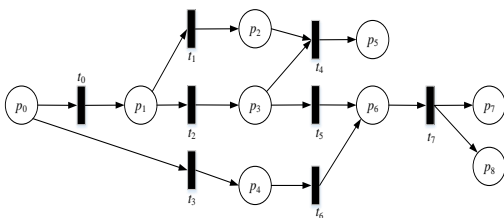


Fig. 4 FPN model

$$H = \begin{matrix} & t_0 & t_1 & t_2 & t_3 & t_4 & t_5 & t_6 & t_7 \\ \begin{matrix} p_0 \\ p_1 \\ p_2 \\ p_3 \\ p_4 \\ p_5 \\ p_6 \\ p_7 \\ p_8 \end{matrix} & \begin{pmatrix} -1 & 0 & 0 & -1 & 0 & 0 & 0 & 0 \\ 1 & -1 & -1 & 0 & 0 & 0 & 0 & 0 \\ 0 & 1 & 0 & 0 & -1 & 0 & 0 & 0 \\ 0 & 0 & 1 & 0 & -1 & -1 & 0 & 0 \\ 0 & 0 & 0 & 1 & 0 & 0 & -1 & 0 \\ 0 & 0 & 0 & 0 & 1 & 0 & 0 & 0 \\ 0 & 0 & 0 & 0 & 0 & 1 & 1 & -1 \\ 0 & 0 & 0 & 0 & 0 & 0 & 0 & 1 \\ 0 & 0 & 0 & 0 & 0 & 0 & 0 & 1 \end{pmatrix} \end{matrix}$$

According to the incidence matrix H , the rules are interpreted as follows:

(1) If a column contains multiple elements with a value of -1, this indicates that the corresponding transition has numerous inputs in the FPN, and the FPR represents an 'AND' rule. For example, the column corresponding to t_5 in the incidence matrix H exemplifies this.

(2) If a row contains multiple elements with a value of 1, it indicates that the corresponding place is the output of several different transitions in the FPN, and the corresponding FPR is an "OR" rule. For example, the row corresponding to p_6 in the incidence matrix H exemplifies this.

(3) If a column contains multiple elements with a value of 1, it indicates that the corresponding transition has multiple outputs in the FPN, which corresponds to the FPN with the disjunctive conclusions rule. For example, the column corresponding to t_7 in the incidence matrix H exemplifies this.

(4) If a row contains multiple elements with a value of -1, it indicates that the place has multiple outputs in the FPN, which corresponds to the FPN with the disjunctive conclusions rule. For example, the row corresponding to p_1 in the incidence matrix H exemplifies this.

2.4 General reasoning algorithm using FPN and related operational operators

According to the references (Gao et al., 2003; Yuan et al., 2008), six operators are frequently used in reasoning using FPN below.

$\oplus: C = A \oplus B \Rightarrow c_{ij} = \max(a_{ij}, b_{ij})$, where A, B , and C are all $n \times m$ fuzzy matrices with a_{ij}, b_{ij} , and c_{ij} being their elements, respectively;

$\otimes: C = A \otimes B \Rightarrow C_{ij} = \max_{1 \leq k \leq l} (a_{ik} \square b_{kj})$, where A, B , and C are $n \times l, l \times m, n \times m$ fuzzy matrices with a_{ij}, b_{ij} , and c_{ij} being their elements, respectively;

$\odot: C = A \odot B \Rightarrow c_{ij} = a_{ij} \cdot b_{ij}$, where A, B , and C are all $n \times m$ fuzzy matrices with a_{ij}, b_{ij} , and c_{ij} being their elements, respectively;

$$\odot: C = A \odot B \Rightarrow \begin{cases} C_{ij} = 1, a_{ij} \geq b_{ij} \\ C_{ij} = 0, a_{ij} < b_{ij} \end{cases}, \text{ where } A, B, \text{ and } C$$

are all $n \times m$ fuzzy matrices with a_{ij} , b_{ij} , and c_{ij} being their elements, respectively;

$\nabla: C = A \nabla B \Rightarrow c_{ij} = \min(a_{ij}, b_{ij})$, where A , B , and C are all fuzzy matrices with a_{ij} , b_{ij} , and c_{ij} being their elements, respectively. More importantly, the elements of the matrix in B are all 1;

$$\oplus: C = \oplus A \Rightarrow \begin{cases} C_{ij} = a_{ij}^{-1}, a_{ij} \neq 0 \\ C_{ij} = 0, a_{ij} = 0 \end{cases}, \text{ where } A \text{ is } n \times m$$

fuzzy matrix.

The general reasoning algorithm using FPN is illustrated in Algorithm 1 below.

Algorithm 1 Formal Reasoning Algorithm by FPN

Input: Initial fuzzy token value M_0 , input matrix I , output matrix O , threshold vector Th .

Output: Final token value M of the places.

Step 1 Initialize the input variables and the number of iterations $k=0$;

Step 2 Calculate the equivalent fuzzy input token value vector E for each transition:

$$E = (I^T \times M_k) \nabla B, \quad (4)$$

where B is an m -dimensional column vector with all elements of 1;

Step 3 Compare the acquired token value vector and threshold vector Th , and remove the input items that cannot fire transitions:

$$G = E \odot (E \odot Th) \quad (5)$$

Step 4 Calculate the token value of the fuzzy output places:

$$S = (O \otimes G) \nabla B \quad (6)$$

Where, B is an m -dimensional column vector with all elements of 1;

Step 5 Calculate the token value for all currently obtained places:

$$M_{k+1} = M_k \oplus S \quad (7)$$

Step 6 If $M_{k+1} \neq M_k$, make $k++$, move to Step 2; otherwise, the reasoning ends, output token value M_{k+1} and the number of iterations k .

3 Reverse FPN and related operations

This section introduces the related concepts of the reverse FPN and the corresponding mapping between the original FPN and reverse FPN. Definitions of reverse nets and reverse FPN are illustrated below.

Definition 8 Reverse PN (Hu et al., 2011).

Let $\Sigma_1 = (P_1, T_1, F_1)$ and $\Sigma_2 = (P_2, T_2, F_2)$ be two PNs; the Σ_2 is the corresponding reverse PN of

Σ_1 if $F_2 = \{(x, y) | (y, x) \in F_1\}$ exists.

According to definition 8, the formalism of the reverse FPN could be given as shown below.

Definition 9 Reverse FPN (Re-FPN).

Let $\Sigma_1 = (P_1, T_1, F_1, M_1, W_1, Th_1, CF_1, I_1, O_1)$ and $\Sigma_2 = (P_2, T_2, F_2, M_2, W_2, Th_2, CF_2, I_2, O_2)$ be two FPNs, Σ_2 is the corresponding Re-FPN of Σ_1 if $P_1 = P_2, T_1 = T_2$, and $F_1 = F_2^{-1}$ exist.

3.1 Correspondence between original FPN and reverse FPN

To derive the corresponding Re-FPN from the original FPN, some key points are considered from various perspectives, including the Re-FPN that corresponds to the simple rule, the Re-FPN that corresponds to the ‘AND’ rule, the Re-FPN that corresponds to the ‘OR’ rule, the Re-FPN with disjunctive conclusions, and the Re-FPN with conjunctive conclusions. Additionally, during the generation of the Re-FPN, a potential issue arises where the input and output arc weights may exceed 1, following reversal operations. To construct a Re-FPN that mirrors the forward reasoning rule, two new matrices in the subsequent section are considered, which are the weight matrix of the input place In and the weight matrix of the output place Out . These matrices are designed to maintain consistency within the transformed net system with the definition of the FPN.

Definition 10 Weight matrix of the input place In

$In = (\alpha(p_i, t_j))_{n \times m}$ is utilized to record the weights associated with the input places. $\alpha(p_i, t_j) = w_{ij}$ when there is a directed arc from p_i to t_j ($i = 1, 2, \dots, n; j = 1, 2, \dots, m$). Otherwise, $\alpha(p_i, t_j) = 0$.

Definition 11 Weight matrix of the output place Out

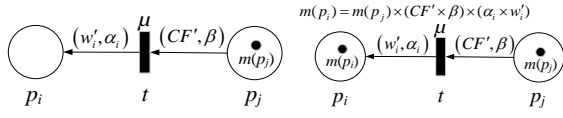
$Out = (\beta(p_i, t_j))_{n \times m}$ is utilized to record the CF_{ij} associated with the output places. $\beta(p_i, t_j) = CF_{ij}$ where there is a directed arc from t_j to p_i ($i = 1, 2, \dots, n; j = 1, 2, \dots, m$). Otherwise $\beta(p_i, t_j) = 0$.

The corresponding Re-FPN generation for the five different types of FPNs is detailed as follows.

(1) Re-FPN corresponds to the simple rule.

The Re-FPN corresponding to the simple FPN is shown in Fig. 5(a). If $m(p_j) \times (CF' \times \beta) \geq \mu$ exists, the transitions can be fired, and the result after fired is $m(p_i) = m(p_j) \times (CF' \times \beta) \times (\alpha_i \times w'_i)$ (Fig. 5(b)), where

$$\alpha_i = \frac{1}{w_i}, w'_i = 1, CF' = 1, \beta = \frac{1}{CF}, i = 1, 2, \dots, n.$$



(a) before transition is fired (b) after transition is fired

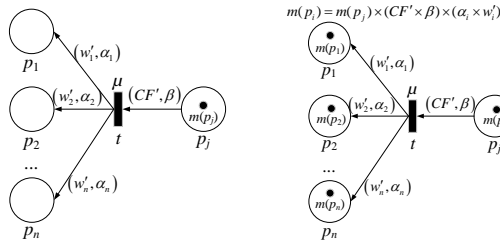
Fig. 5 Re-FPN corresponds to the simple rule

(2) Re-FPN corresponds to the "AND" rule.

The Re-FPN corresponding to the "AND" rule is shown in Fig. 6(a), where the new output weight is $w'_i = \frac{1}{n}$. The transitions can be fired if $m(p_j) \times (CF' \times \beta) \geq \mu$ exists.

The result after being fired is $m(p_i) = m(p_j) \times (CF' \times \beta) \times (\alpha_i \times w'_i)$ (Fig. 6(b)), where

$$\alpha_i = \frac{1}{w_i}, w'_i = \frac{1}{n}, CF'=1, \beta = \frac{1}{CF}, i = 1, 2, \dots, n.$$



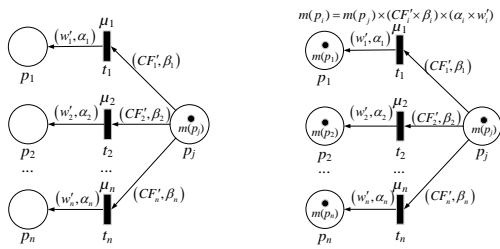
(a) before being fired (b) after being fired

Fig. 6 Re-FPN corresponds to the "AND" rule

(3) Re-FPN corresponds to the "OR" rule.

The Re-FPN corresponding to the "OR" rule is shown in Fig. 7(a). The transitions can be fired if $m(p_j) \times (CF'_i \times \beta_i) \geq \mu_i$ exists. The result after being fired is $m(p_i) = m(p_j) \times (CF'_i \times \beta_i) \times (\alpha_i \times w'_i)$ (Fig. 7(b)),

$$\text{where } \alpha_i = \frac{1}{w_i}, w'_i = 1, CF'_i = 1, \beta_i = \frac{1}{CF_i} (i = 1, 2, \dots, n).$$



(a) before being fired (b) after being fired

Fig. 7 Re-FPN corresponds to the "OR" rule

(4) Re-FPN corresponds to FPN with disjunctive conclusions.

The FPN model with disjunctive conclusions could be understood as consisting of several simple rules with the same preconditions as shown in Fig. 8. Its result after firing in the simple rule way is $m(p_i) = m(p_j) \times w_i \times CF_i$. The corresponding Re-FPN is shown in Fig. 9(a). The transitions can be fired if $m(p_i) \times (CF'_i \times \beta_i) \geq \mu_i$ exists. Moreover, if multiple transitions can be fired simulta-

neously, the fired result takes the maximum value of each output

$$m(p_j) = \max(m(p_i) \times (CF'_i \times \beta_i) \times (\alpha_i \times w'_i)) \quad (\text{Fig. 9(b)}),$$

$$\text{where } \alpha_i = \frac{1}{w_i}, w'_i = 1, CF'_i = 1,$$

$$\beta_i = \frac{1}{CF_i} (i = 1, 2, \dots, n).$$

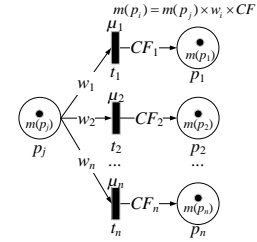
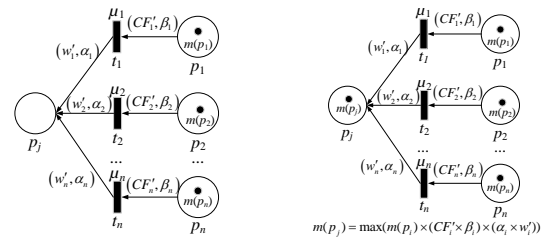


Fig. 8 FPN with disjunctive conclusion



(a) before being fired

(b) after being fired

Fig. 9 Re-FPN corresponds to Fig. 8

(5) Re-FPN corresponds to the FPN with conjunctive conclusions.

The FPN with conjunctive conclusions can be understood as being composed of several simple rules with the same precondition as shown in Fig. 10. Its result after firing in the simple rule way is $m(p_i) = m(p_j) \times w_i \times CF_i$. The corresponding Re-FPN is shown in Fig. 11(a). The transitions can be fired; the fired result is

$$m(p_j) = (\sum m(p_i) \times (CF'_i \times \beta_i)) \times (w'_i \times \alpha_i) \quad \text{if}$$

$$\sum m(p_i) \times (CF'_i \times \beta_i) \geq \mu_i \text{ exists (Fig. 11(b)), where}$$

$$\alpha_i = \frac{1}{w_i}, w'_i = 1, CF'_i = \frac{1}{n}, \beta_i = \frac{1}{CF_i}, i = 1, 2, \dots, n.$$

To satisfy the condition that the sum of the weights of the individual preconditions of the "and" rule is 1, it needs to normalize the input weights after the reverse operation

$$CF'_i = \frac{1}{n}.$$

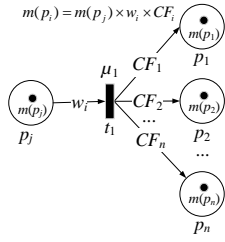
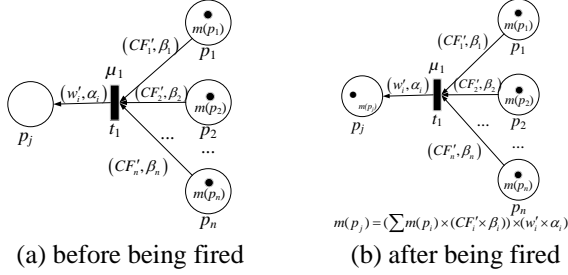


Fig. 10 FPN with the conjunctive rule



(a) before being fired (b) after being fired

Fig. 11 Re-FPN corresponds to Figure 10

3.2 Re-FPN generation algorithm

Due to the mapping relationship, the Re-FPN generation algorithm is demonstrated below.

Algorithm 2 Re-FPN Generation Algorithm

Input: $FPN(\Sigma) = (P_1, T_1, F_1, M, W, Th_1, CF_1, I_1, O_1)$, incidence matrix H ;

Output: Re-FPN's places P_2 , transitions T_2 , flow relationship F_2 , threshold vector Th_2 , confidence matrix CF_2 , input matrix I_2 , output matrix O_2 , weight matrix of the input place In , weight matrix of the output place Out .

Step 1 $P_2 = P_1$, $T_2 = T_1$, $F_2 = F_1^{-1}$;

Step 2 $I_2 = I_3 = H \oplus O_1$;

Step 3 $In = \otimes O_1$;

Step 4 $T' = \{t_i / \text{count}(H(:, i) > 0) > 1\} (i=0, 1, \dots, m-1)$ represents the transition set with the "conjunctive conclusion" rule. Moreover, $\text{count}(H(:, i) > 0)$ denotes the number of elements greater than 0 in column i of the incidence matrix H ;

Step 5 If $\exists t_j \in T'$, $\text{num} = \text{count}(H(:, j) > 0)$,

$I_2(i, j) = \frac{I_3(i, j)}{\text{num}} (i=0, 1, \dots, n-1)$; Otherwise, move to Step 6;

Step 6 $O_2 = O_3 = -H \oplus I_1$;

Step 7 $Out = \otimes I_1$;

Step 8 $T' = \{t_i \mid \text{count}(H(:, i) > 0) > 1\}$

$(i=0, 1, \dots, m-1)$ represents the transition set with the "AND" rule. Moreover, $\text{count}(H(:, i) < 0)$ denotes the number of elements less than 0 in column i of the incidence matrix H ;

Step 9 If $\exists t_j \in T'$, $\text{num} = \text{count}(H(:, i) < 0)$;

$O_2(i, j) = \frac{O_3(i, j)}{\text{num}} (i=0, 1, \dots, n-1)$; Otherwise, move

to Step 10;

Step 10 Threshold vector $Th_2 = Th_1$;

Step 11 Confidence matrix $CF_2 = O_2$;

Step 12 Output Re-FPN's places P_2 , transitions T_2 , flow relationship F_2 , input matrix I_2 , output matrix O_2 , threshold vector Th_2 , confidence matrix CF_2 , weight matrix of the input place In , and weight matrix of the output place Out .

In general, assuming that the FPN has n places and m transitions, the time complexity of Re-FPN generation algorithm is $O(n \times m)$.

4 Parallel bidirectional reasoning algorithm

The main stages of the proposed PBR-HFPN-RDD algorithm are outlined as follows:

(1) Obtain the Hierarchical FPN for subsequent decomposition operations.

(2) Decompose the HFPN into two sub-FPNs: the left-sub-FPN and the right-sub-FPN.

(3) Generate the Re-right-sub-FPN for the right-sub-FPN.

(4) Execute parallel reasoning between the left-sub-FPN and the Re-right-sub-FPN.

4.1 Hierarchical FPN

In some cases, the affiliation relationship between places and transitions in FPNs is not clear. This could lead to confusion regarding the hierarchical structure of the FPN, and make it difficult to determine the sub-FPNs to which the places and transitions belong when decomposing the original FPN. To address this issue, this paper employs the hierarchical algorithm by reverse search (HFPN-RS) to obtain the hierarchical FPN (Xiang et al., 2023).

4.2 Dynamic decomposition of HFPN

For the FPN depicted in Fig. 12, assume that the initial marking is $M_0 = (0.4 \ 0.6 \ 0)^T$. The result of enabling and firing based on the "AND" rule is $M_1 = (0.4 \ 0.6 \ 0.437)^T$. Conversely, the initial marking of the Re-FPN corresponding to the "AND" rule is $M_0 = (0 \ 0 \ 0.437)^T$, and the result after enabling and firing according to the reverse rule is $M_1 = (0.3286 \ 0.7667 \ 0.437)^T$. Clearly, the token values of places p_0 and p_1 obtained through reasoning in the Re-FPN do not align with the original FPN.

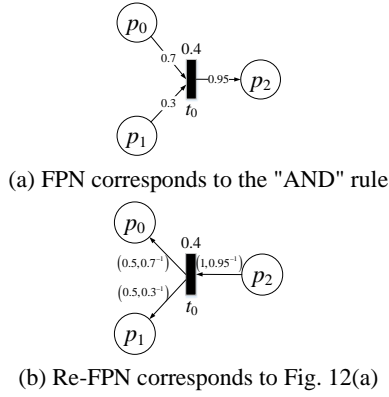


Fig. 12 Example of FPN

Due to the inability to determine the exact weights of the FPN corresponding to the "AND" rule after reversal, it is impractical to obtain fuzzy token values for the Re-FPN that are consistent with the original FPN. This inconsistency becomes the primary source of error in the reasoning process of the Re-FPN. Consequently, this paper proposes a dynamic decomposition strategy for the hierarchical FPN to mitigate the errors in the reasoning process of the Re-FPN. For instance, Fig. 13 illustrates three decomposition strategies for the hierarchical FPN. After executing the HFPN-RS, the sets of transitions for each layer are defined as $T_1=\{t_0, t_1, t_2\}$, $T_2=\{t_3, t_4, t_5\}$, $T_3=\{t_6, t_7\}$, and $T_4=\{t_8\}$, respectively.

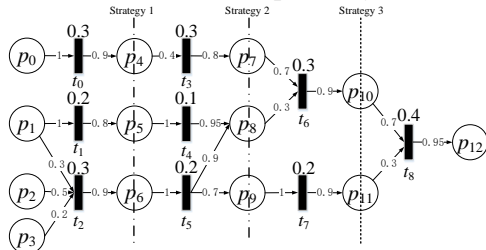


Fig. 13 Different decomposition strategies

Based on the method of distinguishing between different rules, if there are multiple inputs for t_2 within the set $T_1=\{t_0, t_1, t_2\}$, this indicates that the rule corresponds to the "AND" rule. Similarly, the number of "AND" rules within the set T_1 is 1, the number of "AND" rules within the set T_2 is 0, the number of "and" rules within the set T_3 is 1, and the number of "AND" rules within the set T_4 is 1.

If the subsequent set of T_1 is used as the basis for decomposition, as in Decomposition Strategy 1 shown in Fig. 13, it is divided into a left-sub-FPN and a right-sub-FPN. In the right-sub-FPN, as depicted in Fig. 14, there are two "AND" rules.

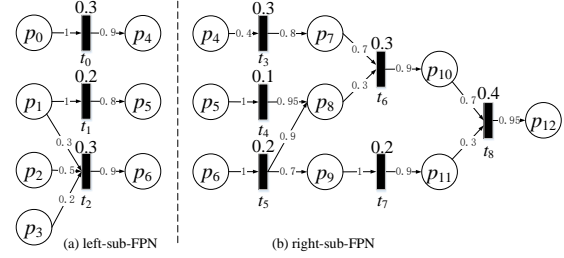


Fig. 14 HFPN model decomposition schematic diagram

If the subsequent set of T_2 is used as the basis for decomposition, as in Decomposition Strategy 2 shown in Fig. 13, it is also divided into a left-sub-FPN and a right-sub-FPN, with the right-sub-FPN containing two "AND" rules.

If the subsequent set of T_3 is used as the basis for decomposition, as in Decomposition Strategy 3 shown in Fig. 13, it is further divided into a left-sub-FPN and a right-sub-FPN, with the right-sub-FPN having only one "AND" rule.

In summary, dynamically decomposing the FPN according to practical needs, such as the size of the FPN or the types of rules in the sub-FPNs, can reduce errors in the reasoning process. Based on the above analysis, the proposed dynamic decomposition algorithm is as follows.

Algorithm 3: Dynamic Decomposition Algorithm of HFPN

Input: HFPN input matrix I , output matrix O , incidence matrix H , the set of variants for each layer $T_k = \{T_1, T_2, \dots, T_k\}$;

Output: left-sub-FPN, right-sub-FPN the input matrices I_1, I_2 , the output matrices O_1, O_2 , and the threshold vectors Th_1, Th_2 .

Step 1. Initialization parameters $A[k]=\{0\}$, $C[k]=\{0\}$;

Step 2. If $k=1$, then the FPN does not need to be decomposed and exits;

Step 3. Counting the number of "AND" rules in each level of the transition set A : If $t_j \in T_i \cup (\text{count}(H(:, j) < 0) > 1)$ ($j = 0, 1, \dots, m-1; i = 1, \dots, k$), then $A[i]=A[i]+1$;

Step 4. Counting the number of "AND" rules in the left-sub-FPN under different decomposition strategies:

$$C[i] = \sum_{j=1}^i A[j] \quad (i = 1, \dots, k);$$

Step 5. The decomposition strategy is determined according to the principles of the minimum

number of "AND" rules and the maximum number of layers in the right-sub-FPN ($R_r \leq \frac{k}{2}$, the R_r denotes the number of layers of the right-sub-FPN);

$$\text{minIndex} = \text{argmin}(C[k] - C[i]) \left(i = \left\lfloor \frac{k}{2} \right\rfloor, \dots, k-1 \right),$$

where $\text{argmin}()$ represents returning the index corresponding to the variable that achieves the minimum value.

Step 6. The elements of the left-sub-FPN are composed of layers $T_1 \sim T_{\text{minIndex}}$ and the pre-set and post-set places of each layer, and the elements of the right-sub-FPN are composed of layers $T_{\text{minIndex}} \sim T_k$ and the pre-set and post-set places of each layer.

Assuming that the HFPN has n places and m transitions, the time complexity of the HFPN dynamic decomposition algorithm is $O(n \times m)$.

4.3 Proposed PBR-HFPN-RDD algorithm

The detailed steps of the PBR-HFPN-RDD algorithm are shown in Algorithm 4.

Algorithm 4 PBR-HFPN-RDD algorithm

Input: Initial marking M_0 , input matrix I , output matrix O , threshold vector Th ;

Output: The fuzzy token value of the predicted initial places ρ_0 and the error value E .

Pre-processing: If there exists a loop structure of FPN, the PBR-HFPN-RDD will be exited automatically;

Step 1 Initialize the input variables, and make the number of iterations $i=0$;

Step 2 Judge whether the hierarchical algorithm is needed for a given FPN and implement the hierarchical operations. Then, update the input matrix I' , output matrix O' , and Th' ;

Step 3 Dynamic decomposition of HFPN using **Algorithm 3** to obtain the left-sub-FPN and right-sub-FPN, the input matrices I_1, I_2 , the output matrices O_1, O_2 and the threshold vectors Th_1, Th_2 ;

Step 4 Generate the Re-right-sub-FPN corresponding to the right-sub-FPN by **Algorithm 2** and obtain the related I'_2, O'_2, Th'_2, In and Out ;

Step 5 Implement **Algorithm 1** on the left-sub-FPN to obtain the inference result θ_i and final value of the output place(s) of the left-sub-FPN V_i ;

Step 6 Get the equivalent weighted input and output place matrices of the Re-right-sub-FPN, which

are $I'_2 = I'_2 \square In$ and $O'_2 = O'_2 \square Out$, respectively. The input place set P_{in} of the Re-right-sub-FPN is also got, where $P_{in} = \{p_0, p_1, \dots, p_{y-1}\}$ and the number of input places is y ;

Step 7 Initialize the initial token value of the Re-right-sub-FPN $\rho_i^{(0)} = (0 \ 0 \ \dots \ 0)^T$;

Step 8 Make the initial token value of the input place p_i equal to 1 and implement **Algorithm 1** on the Re-right-sub-FPN to obtain the inference result in $\theta_r^{(i)}$ and the final value of the output place(s) of the left-sub-FPN $V_r^{(i)}$;

Step 9 Calculate the error in the output places between the left-sub-FPN and Re-right-sub-FPN as

$$E_i = \sqrt{\sum_{j=1}^k (V_{r(j)}^{(i)} - V_{l(j)})^2}, \text{ where } k \text{ is the number of the}$$

output places of sub-FPN;

Step 10 If $i \neq y-1$, make $i=i+1$ and move to step 7; otherwise, output $E_x = \min(E_0, E_1, \dots, E_{y-1})$ and $\rho_x^{(0)}$. The corresponding input place which fulfills $m(p_x)=1$ is the final result of the whole reasoning.

4.4 Algorithm analysis

Assuming there is an FPN without a loop with n places and m transitions, the reasoning executes $h+1$ times under the worst conditions, where h is the number of transitions of the longest path in the FPN.

At the identical time $h \leq m$, the time complexity is $O(n \times m^2)$ for formal reasoning using FPN, $O(m \times (n+m))$ for the hierarchical algorithm, and the size of the FPN increases from $n \times m$ to $(n+r) \times (m+r)$ after performing the hierarchical operation, where r is the number of at least the number of virtual-place–virtual-transition pairs to be added:

$O(n \times m)$ for the HFPN decomposition algorithm;
 $O(n \times m)$ for generation of the Re-right-sub-FPN;

$Max\{O(g \times l^2), O(s \times x \times (n+r-g) \times (m+r-l))\}$ for executing bidirectional reasoning, where g, l, s, x are the left-sub-FPN places number, left-sub-FPN transitions number, the right-sub-FPN reasoning loop times, and right-sub-FPN execution formal reasoning algorithm cycle times, respectively.

Hence, the entire time complexity of the proposed PBR-HFPN-RDD algorithm is

$$\begin{aligned} & O\{m \times (n+m) + n \times m + n \times m + Max\{O(g \times l^2), O(s \times x \times (n+r-g) \times (m+r-l))\}\} \\ & \leq O\{m \times (n+m) + n \times m + n \times m + Max\{O(g \times l^2), O(s \times (m+r) \times (n+r-g) \times (m+r-l))\}\} \\ & \leq O(s \times (n+r) \times (m+r)^2). \end{aligned}$$

To summarize, for a given FPN with n places and m transitions, in the worst case, the time complexity of PBR-HFPN-RDD is $O(s \times (n+r) \times (m+r)^2)$, where s is the number of output places, and r is the number of at least the number of virtual-place–virtual-transition pairs to be added.

5 Experiment and Analysis

Fault diagnosis plays a crucial role in industrial manufacturing equipment and production processes. It is a critical maintenance activity that aims to detect and identify problems in equipment or production lines in a timely manner to reduce downtime, increase production efficiency, and ensure product quality. In this section, an experimental case of fault diagnosis is used to verify the correctness of the proposed algorithm.

Assume that the following rules from the fault diagnosis rule base are listed below.

- R₀: IF d_0 THEN d_5 ($\mu=0.3, CF=0.9, w=1$)
- R₁: IF d_1 THEN d_6 ($\mu=0.2, CF=0.8, w=1$)
- R₂: IF d_1 AND d_2 AND d_3 THEN d_7 ($\mu=0.3, CF=0.9, w_1=0.3, w_2=0.5, w_3=0.2$)
- R₃: IF d_4 AND d_5 THEN d_8 ($\mu=0.3, CF=0.8, w_1=0.6, w_2=0.4$)
- R₄: IF d_6 THEN d_9 ($\mu=0.1, CF=0.95, w=1$)
- R₅: IF d_7 THEN d_9 AND d_{10} ($\mu=0.2, CF_1=0.9, CF_2=0.7, w=1$)
- R₆: IF d_8 AND d_9 THEN d_{11} ($\mu=0.3, CF=0.9, w_1=0.7, w_2=0.3$)
- R₇: IF d_{10} THEN d_{12} AND d_{13} ($\mu=0.2, CF_1=0.9, CF_2=0.8, w=1$)
- R₈: IF d_{11} AND d_{12} THEN d_{14} ($\mu=0.4, CF=0.95, w_1=0.7, w_2=0.3$)
- R₉: IF d_{13} THEN d_{15} ($\mu=0.3, CF=0.8, w=1$)

The corresponding FPN model is generated as shown in Fig. 15 below.

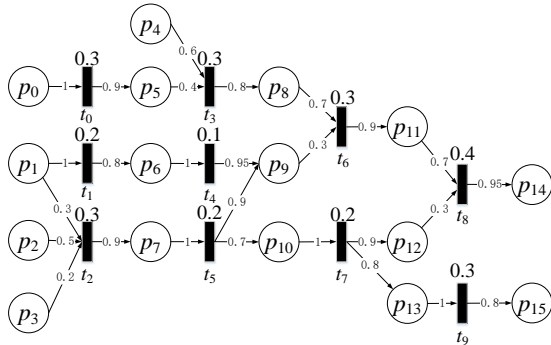


Fig. 15 Corresponding FPN of the given rules

5.1 FPN hierarchical phase

The input matrix I , output matrix O , and threshold vector Th of Fig. 15 are listed below.

$$I = \begin{pmatrix} 1 & 0 & 0 & 0 & 0 & 0 & 0 & 0 & 0 & 0 \\ 0 & 1 & 0.3 & 0 & 0 & 0 & 0 & 0 & 0 & 0 \\ 0 & 0 & 0.5 & 0 & 0 & 0 & 0 & 0 & 0 & 0 \\ 0 & 0 & 0.2 & 0 & 0 & 0 & 0 & 0 & 0 & 0 \\ 0 & 0 & 0 & 0.6 & 0 & 0 & 0 & 0 & 0 & 0 \\ 0 & 0 & 0 & 0.4 & 0 & 0 & 0 & 0 & 0 & 0 \\ 0 & 0 & 0 & 0 & 1 & 0 & 0 & 0 & 0 & 0 \\ 0 & 0 & 0 & 0 & 0 & 1 & 0 & 0 & 0 & 0 \\ 0 & 0 & 0 & 0 & 0 & 0 & 0.7 & 0 & 0 & 0 \\ 0 & 0 & 0 & 0 & 0 & 0 & 0.3 & 0 & 0 & 0 \\ 0 & 0 & 0 & 0 & 0 & 0 & 0 & 1 & 0 & 0 \\ 0 & 0 & 0 & 0 & 0 & 0 & 0 & 0 & 0.7 & 0 \\ 0 & 0 & 0 & 0 & 0 & 0 & 0 & 0 & 0.3 & 0 \\ 0 & 0 & 0 & 0 & 0 & 0 & 0 & 0 & 0 & 1 \\ 0 & 0 & 0 & 0 & 0 & 0 & 0 & 0 & 0 & 0 \\ 0 & 0 & 0 & 0 & 0 & 0 & 0 & 0 & 0 & 0 \end{pmatrix}$$

$$O = \begin{pmatrix} 0 & 0 & 0 & 0 & 0 & 0 & 0 & 0 & 0 & 0 \\ 0 & 0 & 0 & 0 & 0 & 0 & 0 & 0 & 0 & 0 \\ 0 & 0 & 0 & 0 & 0 & 0 & 0 & 0 & 0 & 0 \\ 0 & 0 & 0 & 0 & 0 & 0 & 0 & 0 & 0 & 0 \\ 0.9 & 0 & 0 & 0 & 0 & 0 & 0 & 0 & 0 & 0 \\ 0 & 0.8 & 0 & 0 & 0 & 0 & 0 & 0 & 0 & 0 \\ 0 & 0 & 0.9 & 0 & 0 & 0 & 0 & 0 & 0 & 0 \\ 0 & 0 & 0 & 0.8 & 0 & 0 & 0 & 0 & 0 & 0 \\ 0 & 0 & 0 & 0 & 0.95 & 0.9 & 0 & 0 & 0 & 0 \\ 0 & 0 & 0 & 0 & 0 & 0.7 & 0 & 0 & 0 & 0 \\ 0 & 0 & 0 & 0 & 0 & 0 & 0.9 & 0 & 0 & 0 \\ 0 & 0 & 0 & 0 & 0 & 0 & 0 & 0.9 & 0 & 0 \\ 0 & 0 & 0 & 0 & 0 & 0 & 0 & 0 & 0.8 & 0 \\ 0 & 0 & 0 & 0 & 0 & 0 & 0 & 0 & 0 & 0.95 \\ 0 & 0 & 0 & 0 & 0 & 0 & 0 & 0 & 0 & 0.8 \end{pmatrix}$$

$$Th = (0.3 \ 0.2 \ 0.3 \ 0.3 \ 0.1 \ 0.2 \ 0.3 \ 0.2 \ 0.4 \ 0.3)^T$$

The FPN is translated into HFPN with a clear structure by executing a hierarchical algorithm to increase the virtual place p_{16} and the virtual transitions t_{10} with three decomposition strategies, as shown in Fig. 16. The threshold of virtual transitions is 0, and the virtual transitions to the post-set place have a confidence degree of 1, i.e., $CF(t, t^*) \equiv 1$.

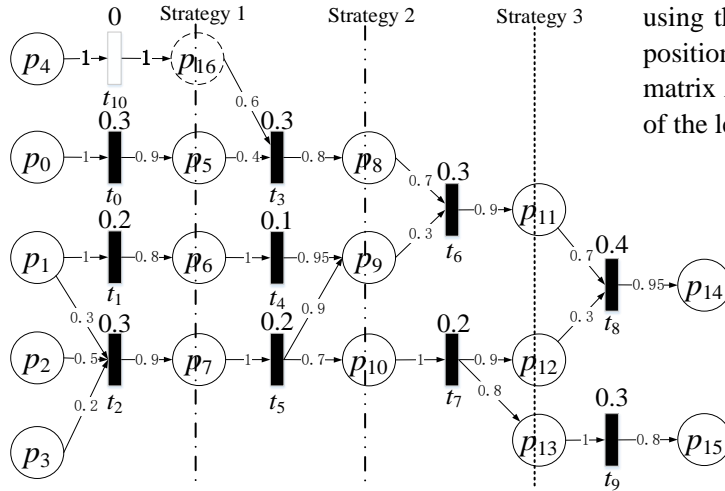


Fig. 16 FPN with hierarchical structure

The input matrix I' , output matrix O' , and threshold vector Th' of the HFPN are obtained below.

$$I' = \begin{pmatrix} 1 & 0 & 0 & 0 & 0 & 0 & 0 & 0 & 0 & 0 & 0 & 0 & 0 & 0 & 0 & 0 \\ 0 & 1 & 0.3 & 0 & 0 & 0 & 0 & 0 & 0 & 0 & 0 & 0 & 0 & 0 & 0 & 0 \\ 0 & 0 & 0.5 & 0 & 0 & 0 & 0 & 0 & 0 & 0 & 0 & 0 & 0 & 0 & 0 & 0 \\ 0 & 0 & 0.2 & 0 & 0 & 0 & 0 & 0 & 0 & 0 & 0 & 0 & 0 & 0 & 0 & 0 \\ 0 & 0 & 0 & 0 & 0 & 0 & 0 & 0 & 0 & 0 & 0 & 0 & 0 & 0 & 0 & 1 \\ 0 & 0 & 0 & 0.4 & 0 & 0 & 0 & 0 & 0 & 0 & 0 & 0 & 0 & 0 & 0 & 0 \\ 0 & 0 & 0 & 0 & 1 & 0 & 0 & 0 & 0 & 0 & 0 & 0 & 0 & 0 & 0 & 0 \\ 0 & 0 & 0 & 0 & 0 & 1 & 0 & 0 & 0 & 0 & 0 & 0 & 0 & 0 & 0 & 0 \\ 0 & 0 & 0 & 0 & 0 & 0 & 0 & 0.7 & 0 & 0 & 0 & 0 & 0 & 0 & 0 & 0 \\ 0 & 0 & 0 & 0 & 0 & 0 & 0 & 0.3 & 0 & 0 & 0 & 0 & 0 & 0 & 0 & 0 \\ 0 & 0 & 0 & 0 & 0 & 0 & 0 & 0 & 0 & 0 & 1 & 0 & 0 & 0 & 0 & 0 \\ 0 & 0 & 0 & 0 & 0 & 0 & 0 & 0 & 0 & 0 & 0 & 0.7 & 0 & 0 & 0 & 0 \\ 0 & 0 & 0 & 0 & 0 & 0 & 0 & 0 & 0 & 0 & 0 & 0.3 & 0 & 0 & 0 & 0 \\ 0 & 0 & 0 & 0 & 0 & 0 & 0 & 0 & 0 & 0 & 0 & 0 & 0 & 1 & 0 & 0 \\ 0 & 0 & 0 & 0 & 0 & 0 & 0 & 0 & 0 & 0 & 0 & 0 & 0 & 0 & 0 & 0 \\ 0 & 0 & 0 & 0 & 0 & 0 & 0 & 0 & 0 & 0 & 0 & 0 & 0 & 0 & 0 & 0 \\ 0 & 0 & 0 & 0 & 0 & 0 & 0 & 0 & 0 & 0 & 0 & 0 & 0 & 0 & 0 & 0 \\ 0 & 0 & 0 & 0 & 0.6 & 0 & 0 & 0 & 0 & 0 & 0 & 0 & 0 & 0 & 0 & 0 \end{pmatrix}$$

$$O' = \begin{pmatrix} 0 & 0 & 0 & 0 & 0 & 0 & 0 & 0 & 0 & 0 & 0 & 0 & 0 & 0 & 0 & 0 \\ 0 & 0 & 0 & 0 & 0 & 0 & 0 & 0 & 0 & 0 & 0 & 0 & 0 & 0 & 0 & 0 \\ 0 & 0 & 0 & 0 & 0 & 0 & 0 & 0 & 0 & 0 & 0 & 0 & 0 & 0 & 0 & 0 \\ 0 & 0 & 0 & 0 & 0 & 0 & 0 & 0 & 0 & 0 & 0 & 0 & 0 & 0 & 0 & 0 \\ 0.9 & 0 & 0 & 0 & 0 & 0 & 0 & 0 & 0 & 0 & 0 & 0 & 0 & 0 & 0 & 0 \\ 0 & 0.8 & 0 & 0 & 0 & 0 & 0 & 0 & 0 & 0 & 0 & 0 & 0 & 0 & 0 & 0 \\ 0 & 0 & 0.9 & 0 & 0 & 0 & 0 & 0 & 0 & 0 & 0 & 0 & 0 & 0 & 0 & 0 \\ 0 & 0 & 0 & 0.8 & 0 & 0 & 0 & 0 & 0 & 0 & 0 & 0 & 0 & 0 & 0 & 0 \\ 0 & 0 & 0 & 0 & 0.95 & 0.9 & 0 & 0 & 0 & 0 & 0 & 0 & 0 & 0 & 0 & 0 \\ 0 & 0 & 0 & 0 & 0 & 0.7 & 0 & 0 & 0 & 0 & 0 & 0 & 0 & 0 & 0 & 0 \\ 0 & 0 & 0 & 0 & 0 & 0 & 0 & 0.9 & 0 & 0 & 0 & 0 & 0 & 0 & 0 & 0 \\ 0 & 0 & 0 & 0 & 0 & 0 & 0 & 0 & 0.9 & 0 & 0 & 0 & 0 & 0 & 0 & 0 \\ 0 & 0 & 0 & 0 & 0 & 0 & 0 & 0 & 0 & 0.8 & 0 & 0 & 0 & 0 & 0 & 0 \\ 0 & 0 & 0 & 0 & 0 & 0 & 0 & 0 & 0 & 0 & 0.95 & 0 & 0 & 0 & 0 & 0 \\ 0 & 0 & 0 & 0 & 0 & 0 & 0 & 0 & 0 & 0 & 0 & 0 & 0.8 & 0 & 0 & 0 \\ 0 & 0 & 0 & 0 & 0 & 0 & 0 & 0 & 0 & 0 & 0 & 0 & 0 & 0 & 1 & 0 \end{pmatrix}$$

$$Th' = (0 \ 0.3 \ 0.2 \ 0.3 \ 0.3 \ 0.1 \ 0.2 \ 0.3 \ 0.2 \ 0.4 \ 0.3)^T$$

5.2 HFPN decomposition phase and Re-FPN generation phase

To reduce the error in the reasoning, the right-sub-FPN with fewer "AND" rules is obtained

using the decomposition strategy 2, and the decomposition results are shown in Fig. 17(a-b). The input matrix I_1 , output matrix O_1 , and threshold vector Th_1 of the left-sub-FPN are obtained below.

$$I_1 = \begin{pmatrix} 1 & 0 & 0 & 0 & 0 & 0 & 0 & 0 & 0 & 0 \\ 0 & 1 & 0 & 0 & 0 & 0 & 0 & 0 & 0 & 0 \\ 0 & 0 & 1 & 0.3 & 0 & 0 & 0 & 0 & 0 & 0 \\ 0 & 0 & 0 & 0.5 & 0 & 0 & 0 & 0 & 0 & 0 \\ 0 & 0 & 0 & 0.2 & 0 & 0 & 0 & 0 & 0 & 0 \\ 0 & 0 & 0 & 0 & 0.6 & 0 & 0 & 0 & 0 & 0 \\ 0 & 0 & 0 & 0 & 0.4 & 0 & 0 & 0 & 0 & 0 \\ 0 & 0 & 0 & 0 & 0 & 0 & 1 & 0 & 0 & 0 \\ 0 & 0 & 0 & 0 & 0 & 0 & 0 & 1 & 0 & 0 \\ 0 & 0 & 0 & 0 & 0 & 0 & 0 & 0 & 0 & 0.7 \\ 0 & 0 & 0 & 0 & 0 & 0 & 0 & 0 & 0 & 0.3 \\ 0 & 0 & 0 & 0 & 0 & 0 & 0 & 0 & 0 & 0 \\ 0 & 0 & 0 & 0 & 0 & 0 & 0 & 0 & 0 & 0 \\ 0 & 0 & 0 & 0 & 0 & 0 & 0 & 0 & 0 & 0 \\ 0 & 0 & 0 & 0 & 0 & 0 & 0 & 0 & 0 & 0 \end{pmatrix}$$

$$O_1 = \begin{pmatrix} 0 & 0 & 0 & 0 & 0 & 0 & 0 & 0 & 0 & 0 \\ 0 & 0 & 0 & 0 & 0 & 0 & 0 & 0 & 0 & 0 \\ 0 & 0 & 0 & 0 & 0 & 0 & 0 & 0 & 0 & 0 \\ 0 & 0 & 0 & 0 & 0 & 0 & 0 & 0 & 0 & 0 \\ 0 & 0 & 0 & 0 & 0 & 0 & 0 & 0 & 0 & 0 \\ 0 & 0 & 0 & 0 & 0 & 0 & 0 & 0 & 0 & 0 \\ 1 & 0 & 0 & 0 & 0 & 0 & 0 & 0 & 0 & 0 \\ 0 & 0.9 & 0 & 0 & 0 & 0 & 0 & 0 & 0 & 0 \\ 0 & 0 & 0.8 & 0 & 0 & 0 & 0 & 0 & 0 & 0 \\ 0 & 0 & 0 & 0.9 & 0 & 0 & 0 & 0 & 0 & 0 \\ 0 & 0 & 0 & 0 & 0.8 & 0 & 0 & 0 & 0 & 0 \\ 0 & 0 & 0 & 0 & 0 & 0.95 & 0.9 & 0 & 0 & 0 \\ 0 & 0 & 0 & 0 & 0 & 0 & 0 & 0.7 & 0 & 0 \\ 0 & 0 & 0 & 0 & 0 & 0 & 0 & 0 & 0 & 0.9 \\ 0 & 0 & 0 & 0 & 0 & 0 & 0 & 0 & 0 & 0.9 \\ 0 & 0 & 0 & 0 & 0 & 0 & 0 & 0 & 0 & 0.8 \end{pmatrix}$$

$$Th_1 = (0 \ 0.3 \ 0.2 \ 0.3 \ 0.3 \ 0.1 \ 0.2 \ 0.3 \ 0.2)^T$$

Then, the right-sub-FPN will be transformed into a corresponding Re-right-sub-FPN by executing Algorithm 2, and the results are shown in Fig. 17(d). The input matrix I_2' , output matrix O_2' , threshold vector Th_2' , input places weight matrix In , and output places weight matrix Out of the right-sub-FPN are obtained below.

$$I_2' = \begin{pmatrix} 1 & 0 \\ 0 & 1 \\ 0 & 0 \\ 0 & 0 \\ 0 & 0 \end{pmatrix} \quad O_2' = \begin{pmatrix} 0 & 0 \\ 0 & 0 \\ 0.5 & 0 \\ 0.5 & 0 \\ 0 & 1 \end{pmatrix} \quad In = \begin{pmatrix} 0.95^{-1} & 0 \\ 0 & 0.8^{-1} \\ 0 & 0 \\ 0 & 0 \\ 0 & 0 \end{pmatrix} \quad Out = \begin{pmatrix} 0 & 0 \\ 0 & 0 \\ 0.7^{-1} & 0 \\ 0.3^{-1} & 0 \\ 0 & 1 \end{pmatrix}$$

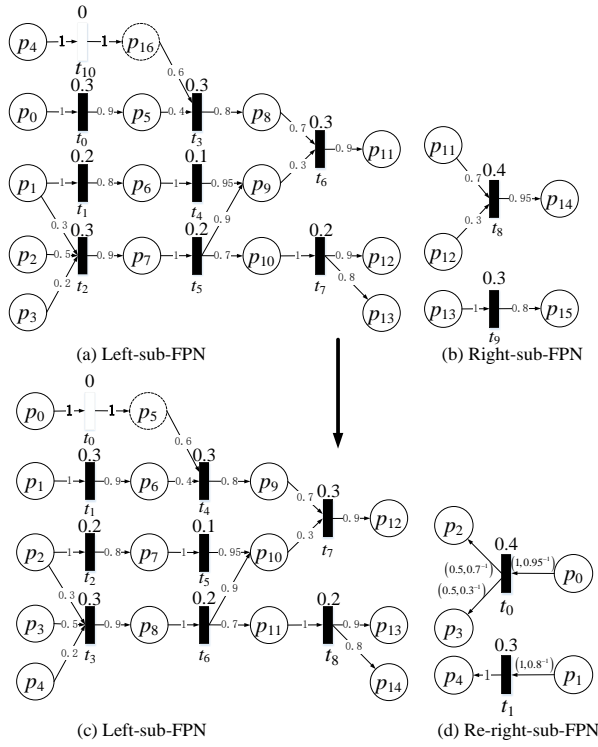


Fig. 17 HFPN decomposition process

5.3 Parallel reasoning phase

Assume that the starting vector M_0 for the given left-sub-FPN is $M_0=(0.5 \ 0.85 \ 0.7 \ 0.75 \ 0.7 \ 0 \ 0 \ 0 \ 0 \ 0 \ 0 \ 0 \ 0 \ 0 \ 0 \ 0)^T$. The final result of running the reasoning algorithm is $M=(0.5 \ 0.85 \ 0.7 \ 0.75 \ 0.7 \ 0.5 \ 0.765 \ 0.56 \ 0.6525 \ 0.4848 \ 0.58725 \ 0.45675 \ 0.463982 \ 0.411075 \ 0.3654)^T$; the final result of executing the formal reasoning algorithm is $(0.463982 \ 0.411075 \ 0.3654)^T$.

Assume that the initial token value of the Re-right-sub-FPN is: $\rho^{(0)}=(1 \ 0 \ 0 \ 0 \ 0)^T$, i.e., p_0 has the maximum probability of fault. The final result of running the reasoning algorithm on the Re-right-sub-FPN could be gained as $\rho=(1 \ 0 \ 0.793651 \ 1 \ 0)^T$.

The final token value of the output places of Re-right-sub-FPN is $(0.793651 \ 1 \ 0)^T$. The final error value of the token value is

$$E_1 = \sqrt{\sum_{j=1}^k (V_{r(j)}^{(i)} - V_{l(j)})^2} = 0.737070.$$

Next, assume that the initial token value of the Re-right-sub-FPN is: $\rho^{(0)}=(0 \ 1 \ 0 \ 0 \ 0)^T$, i.e., p_1 has the maximum probability of fault. The final result of running the reasoning algorithm on the Re-right-sub-FPN could be gained: $\rho=(0 \ 1 \ 0 \ 0 \ 1)^T$. The final token value of the output places of the

Re-right-sub-FPN is $(0 \ 0 \ 1)^T$.

The final error value of the token value is:

$$E_2 = \sqrt{\sum_{j=1}^k (V_{r(j)}^{(i)} - V_{l(j)})^2} = 0.887118.$$

Because of the error value $E_1 < E_2$, it further indicates that the initial place p_0 has a greater probability. The reasoning is terminated, and the result is obtained.

Since the time complexity of the formal reasoning algorithm and the bidirectional reasoning algorithm are both related to the matrix dimension, i.e., the larger the matrix dimension, the greater the time complexity. Table 1 lists a simple comparison among the scale of matrices of various FPNs.

Table 1 Matrix dimension comparison

	Related Matrices	Experiment
Matrices of Original FPN	I AND O	16×10
Matrices of hierarchical FPN	I' AND O'	17×11
Matrices of left-sub-FPN	I_l AND O_l	15×9
Matrices of Re-FPN-right-sub-FPN	I_2' AND O_2'	5×2

In Table 2, it is easy to find that the scale of the operation matrix is compressed, the scale of the original FPN matrix is 16×10 , the scale of the left-sub-FPN is 15×9 , and the scale of the Re-FPN-right-sub-FPN is 5×2 after executing the PBR-HFPN-RDD algorithm. Therefore, when performing bidirectional parallel reasoning, the matrix size of both the left-sub-FPN and the Re-right-sub-FPN is smaller than the size of the original FPN matrix, which effectively compresses the dimensionality of the operation matrix, reduces the time complexity of the algorithm, and improves the reasoning efficiency.

6 Conclusion and future work

In this paper, a bidirectional parallel reasoning algorithm for FPN with a focus on time complexity is proposed. Initially, the correspondence between each element of the reversed FPN and the original FPN is explored from the perspective of the fuzzy production rules. The enabling and firing rules specific to the

reversed FPN are discussed in depth, and an algorithm for generating the reversed FPN (Algorithm 2) is introduced. Subsequently, a dynamic decomposition algorithm (Algorithm 3) is employed to mitigate the presence of excessive “AND” operations in the right-sub-FPN and to decrease the reasoning error within the FPN. Finally, a PBR-HFPN-RDD algorithm (Algorithm 4) is developed based on the aforementioned algorithms to facilitate a bidirectional parallel inference mechanism, addressing the challenge of state explosion. The case study demonstrates that the proposed algorithm significantly reduces the state explosion problem and enhances reasoning efficiency by diminishing the size of the FPN. The reasoning algorithm presented in this paper offers a novel approach to enhancing the decision-making efficiency of large-scale fault diagnosis systems.

While the proposed PBR-HFPN-RDD algorithm provides a genuine parallel inference method using the FPN to resolve the state explosion issue and yields favorable outcomes, several aspects deserve future investigation. Firstly, in FPNs, the “AND” rule necessitates the concurrent satisfaction of all input transitions to trigger an output transition. Variations in weights signify different levels of influence of input transitions on output transition triggering. Due to this attribute, a discrepancy may arise between the token values of places activated by transitions in the reversed net and those in the original net during reasoning. Consequently, our ongoing research aims to employ techniques such as soft computing to refine parameters, including the weights of directed arcs, thereby minimizing reasoning errors. Secondly, the development of more adaptable, potent, and user-friendly tools to illustrate bidirectional reasoning processes is necessary. Thirdly, the proposed bidirectional reasoning algorithm should be applied to other types of high-level network systems to broaden its application scope. Finally, the efficacy and validity of the proposed algorithm should be further tested within more complex rule-based systems.

Acknowledgements: This research is supported by the National Natural Science Foundation of China under grant numbers 62066016, the Natural Science Foundation of Hunan Province of China under Grant 2023JJ2279, the Scientific Research Project of Education Department of Hunan Province of China under

grant numbers 22B0549 and 22C0282, the Post-graduate Scientific Research Innovation Project of Hunan Province under grant number CX20231088, the Fundamental Research Grant Scheme of Malaysia under grant number R.J130000.7809.5F524, and the UTMFR Grant Research Management Center (RMC) of Universiti Teknologi Malaysia (UTM) under grant number Q.J130000.2551.20H71.

Contributors

Yin-Hong Xiang designed the algorithm, drafted the manuscript, and finalized the paper. Di-Wen Kang helped organize the manuscript. Arezoo Sarkheyli-Hägele, Yulsiza Yusoff, and Azlan Mohd Zain revised the paper. Kai-Qing Zhou conceptualized the main idea and led the research. All the authors had in-depth discussions.

Compliance with ethics guidelines

All authors declare that they have no conflict of interest.

References

- Bai KY, Jia D, Meng WY, et al., 2023. Q-rung orthopair fuzzy Petri nets for knowledge representation and reasoning. *IEEE Access*, 11:93560-93573. <https://doi.org/10.1109/ACCESS.2023.3309663>
- Chen RH, Yang B, Li S, et al., 2020. A self-learning genetic algorithm based on reinforcement learning for flexible job-shop scheduling problem. *Comput Ind Eng*, 149:106778. <https://doi.org/10.1016/j.cie.2020.106778>
- Chen SM, 2000. Fuzzy backward reasoning using fuzzy Petri nets. *IEEE Trans Syst, Man, Cybern, Part B (Cybern)*, 30(6):846-856. <https://doi.org/10.1109/3477.891146>
- Chen SM, 2002. Weighted fuzzy reasoning using weighted fuzzy Petri nets. *IEEE Trans Knowl Data Eng*, 14(2):386-397. <https://doi.org/10.1109/69.991723>
- Chen XH, Zhang BK, Gao D, 2021. Bearing fault diagnosis base on multi-scale CNN and LSTM model. *J Intell Manuf*, 32(4):971-987. <https://doi.org/10.1007/s10845-020-01600-2>
- Gao MM, Zhou MC, Huang XG, et al., 2003. Fuzzy reasoning Petri nets. *IEEE Trans Syst, Man, Cybern - Part A: Syst Hum*, 33(3):314-324. <https://doi.org/10.1109/tsmca.2002.804362>
- Grobelna I, Karatkevich A, 2021. Challenges in application of Petri nets in manufacturing systems. *Electronics*, 10(18):2305. <https://doi.org/10.3390/electronics10182305>
- Hu HS, Li ZW, Al-Ahmari A, 2011. Reversed fuzzy Petri nets and their application for fault diagnosis. *Comput Ind Eng*, 60(4):505-510. <https://doi.org/10.1016/j.cie.2010.12.003>
- Jiang W, Zhou KQ, Sarkheyli-Hägele A, et al., 2022. Modeling, reasoning, and application of fuzzy Petri net model: a survey. *Artif Intell Rev*, 55(8):6567-6605. <https://doi.org/10.1007/s10462-022-10161-0>

- Lakos C, Petrucci L, 2011. Modular state spaces for prioritised Petri nets. In: Calinescu R, Jackson E (Eds.), *Foundations of Computer Software*. Springer, Berlin, Heidelberg, p.136-156. https://doi.org/10.1007/978-3-642-21292-5_8
- Lei YG, Yang B, Jiang XW, et al., 2020. Applications of machine learning to machine fault diagnosis: a review and roadmap. *Mech Syst Signal Process*, 138:106587. <https://doi.org/10.1016/j.ymsp.2019.106587>
- Liu HC, Lin QL, Ren ML, 2013. Fault diagnosis and cause analysis using fuzzy evidential reasoning approach and dynamic adaptive fuzzy Petri nets. *Comput Ind Eng*, 66(4):899-908. <https://doi.org/10.1016/j.cie.2013.09.004>
- Liu HC, You JX, Li ZW, et al., 2017. Fuzzy Petri nets for knowledge representation and reasoning: a literature review. *Eng Appl Artif Intell*, 60:45-56. <https://doi.org/10.1016/j.engappai.2017.01.012>
- Liu HC, Luan X, Zhou MC, et al., 2022. A new linguistic Petri net for complex knowledge representation and reasoning. *IEEE Trans Knowl Data Eng*, 34(3):1011-1020. <https://doi.org/10.1109/TKDE.2020.2997175>
- Mou X, Mao LX, Liu HC, et al., 2022. Spherical linguistic Petri nets for knowledge representation and reasoning under large group environment. *IEEE Trans Artif Intell*, 3(3):402-413. <https://doi.org/10.1109/TAI.2022.3140282>
- Nishi T, Matsumoto I, 2015. Petri net decomposition approach to deadlock-free and non-cyclic scheduling of dual-armed cluster tools. *IEEE Trans Autom Sci Eng*, 12(1):281-294. <https://doi.org/10.1109/TASE.2013.2292572>
- Rudin C, 2019. Stop explaining black box machine learning models for high stakes decisions and use interpretable models instead. *Nat Mach Intell*, 1(5):206-215. <https://doi.org/10.1038/s42256-019-0048-x>
- Russell SJ, Norvig P, 2009. *Artificial Intelligence: a Modern Approach*. 3rd ed. Prentice Hall Press, Upper Saddle River, USA.
- Salum L, 2015. Avoiding state explosion in a class of Petri nets. *Expert Syst Appl*, 42(1):519-526. <https://doi.org/10.1016/j.eswa.2014.07.037>
- Seatzu C, 2019. Modeling, analysis, and control of automated manufacturing systems using Petri nets. *Proc 24th IEEE Int Conf on Emerging Technologies and Factory Automation*, p.27-30. <https://doi.org/10.1109/ETFA.2019.8869012>
- Shen VRL, Chung YF, Chen SM, et al., 2013. A novel reduction approach for Petri net systems based on matching theory. *Expert Syst Appl*, 40(11):4562-4576. <https://doi.org/10.1016/j.eswa.2013.01.057>
- Shi H, Liu HC, Wang JH, et al., 2022. New linguistic Z-number Petri nets for knowledge acquisition and representation under large group environment. *Int J Fuzzy Syst*, 24(8):3483-3500. <https://doi.org/10.1007/s40815-022-01341-9>
- Shi H, Yu YX, Liu R, et al., 2024. Probabilistic linguistic Petri nets for knowledge representation and acquisition with dynamic consensus reaching process. *IEEE Trans Fuzzy Syst*, 32(4):2198-2210. <https://doi.org/10.1109/TFUZZ.2023.3347436>
- Valmari A, 1998. The state explosion problem. In: Reisig W, Rozenberg G (Eds.), *Lectures on Petri Nets I: Basic Models*. Springer, Berlin, Heidelberg, p.429-528. https://doi.org/10.1007/3-540-65306-6_21
- Wang XL, Lu FM, Zhou MC, et al., 2022. A synergy-effect-incorporated fuzzy Petri net modeling paradigm with application in risk assessment. *Expert Syst Appl*, 199:117037. <https://doi.org/10.1016/j.eswa.2022.117037>
- Xiang YH, Zhou KQ, Yang SY, et al., 2023. Hierarchical algorithm of fuzzy Petri net by reverse search. *J Comput Appl*, 43(12):3676-3682 (in Chinese). <https://doi.org/10.11772/j.issn.1001-9081.2022121851>
- Yang X, 2023. Performance analysis of Petri net based on moment generating function. *J Intell Fuzzy Syst*, 45(1):1131-1139. <https://doi.org/10.3233/JIFS-231137>
- Ye SQ, Zhou KQ, Zain AM, et al., 2023. A modified harmony search algorithm and its applications in weighted fuzzy production rule extraction. *Front Inf Technol Electron Eng*, 24(11):1574-1590. <https://doi.org/10.1631/FITEE.2200334>
- Yeung DS, Ysang ECC, 1998. A multilevel weighted fuzzy reasoning algorithm for expert systems. *IEEE Trans Syst, Man, Cybern - Part A: Syst Hum*, 28(2):149-158. <https://doi.org/10.1109/3468.661144>
- Yu YX, Gong HP, Liu HC, et al., 2023. Knowledge representation and reasoning using fuzzy Petri nets: a literature review and bibliometric analysis. *Artif Intell Rev*, 56(7):6241-6265. <https://doi.org/10.1007/s10462-022-10312-3>
- Yuan J, Shi HB, Liu C, et al., 2008. Improved basic inference models of fuzzy Petri nets. *Proc 7th World Congress on Intelligent Control and Automation*, p.1488-1493. <https://doi.org/10.1109/WCICA.2008.4593140>
- Zaitsev DA, 2004. Decomposition of Petri nets. *Cybern Syst Anal*, 40(5):739-746. <https://doi.org/10.1007/s10559-005-0012-0>
- Zeng RF, Jiang YX, Lin C, et al., 2012. Dependability analysis of control center networks in smart grid using stochastic petri nets. *IEEE Trans Parallel Distrib Syst*, 23(9):1721-1730. <https://doi.org/10.1109/TPDS.2012.68>
- Zhou KQ, Zain AM, 2016. Fuzzy Petri nets and industrial applications: a review. *Artif Intell Rev*, 45(4):405-446. <https://doi.org/10.1007/s10462-015-9451-9>
- Zhou KQ, Zain AM, Mo LP, 2015a. A decomposition algorithm of fuzzy Petri net using an index function and incidence matrix. *Expert Syst Appl*, 42(8):3980-3990. <https://doi.org/10.1016/j.eswa.2014.12.048>
- Zhou KQ, Zain AM, Mo LP, 2015b. Dynamic properties of fuzzy Petri net model and related analysis. *J Central South Univ*, 22(12):4717-4723. <https://doi.org/10.1007/s11771-015-3023-7>
- Zhou KQ, Gui WH, Mo LP, et al., 2018. A bidirectional diagnosis algorithm of fuzzy Petri net using inner-reasoning-path. *Symmetry*, 10(6):192.

<https://doi.org/10.3390/sym10060192>

Zhou KQ, Mo LP, Jin J, et al., 2019. An equivalent generating algorithm to model fuzzy Petri net for knowledge-based system. *J Intell Manuf*, 30(4):1831-1842.

<https://doi.org/10.1007/s10845-017-1355-x>

Ziani R, Felkaoui A, Zegadi R, 2017. Bearing fault diagnosis using multiclass support vector machines with binary particle swarm optimization and regularized Fisher's criterion. *J Intell Manuf*, 28(2):405-417.

<https://doi.org/10.1007/s10845-014-0987-3>